JETIR.ORG ISSN: 2349-5162 | ESTD Year : 2014 | Monthly Issue
JOURNAL OF EMERGING TECHNOLOGIES AND INNOVATIVE RESEARCH (JETIR)
An International Scholarly Open Access, Peer-reviewed, Refereed Journal

NUMERICAL SIMULATION OF THE EVOLUTION PHOTOREFRACTIVE GAIN IN $BaTiO_3$: Rh

[1] B. Ifegous, [1]J. Farhane, [1]W. Zibar, [2]A. Drighil, [1]T. Lachhab, [1]R. Adhiri

[1]Laboratory of Engineering and Materials (LIMAT), Hassan II University of Casablanca, Faculty of Sciences Ben M'sik, B.P. 7955, Casablanca, Morocco, [2]Laboratory of Information Treatment (LTI), Hassan II University of Casablanca, Faculty of Sciences Ben M'sik,
[1]Physics department
[1]Hassan II University of Casablanca, Faculty of Sciences Ben M'sik, Casablanca, Morocco
Email : b_ifegous@hotmail.com

Abstract:
Oxide perovskites with general formula of ABO_3 are probably the most interesting and technologically important class of materials in manufacture of various microelectronic and optoelectronic. Barium titanate ($BaTiO_3$) is one of the oxide perovskite that has attracted research groups all over the world.
The present work deals with photorefractive gain in $BaTiO_3$: Rh. The photorefractive gain in $BaTiO_3$: Rh is calculated versus the frequency of the applied electric field (in the complex plane and versus time). This numerical calculation is done in terms of a three state-of-charge transport model.

IndexTerms **- Charge transport model, Space charge field, Photorefractive gain, BaTiO3: Rh, Frequency behavior, Energy-level.**

I. INTRODUCTION

Barium titanate ($BaTiO_3$) is a class of ceramic multifunctional materials with unique thermal stability, prominent piezoelectricity constant, excellent dielectric constant, environmental friendliness, and excellent photocatalytic activities. These features have rendered barium titanate indispensable in many areas of applications such as electromechanical devices, thermistors, multilayer capacitors, and electrooptical devices [1,2,3]. In nonlinear optics, barium titanate crystals exhibit high beam coupling gain and can be used at visible spectrum [2] and near infrared wavelengths [4,5]. For photorefractive applications, barium titanate can be doped with various other elements, such as Fe and Rh [6].

Moisan et al [7,8] presented two-wave mixing results obtained with CdTe: V photorefractive crystals under a square-shaped alternating electric field. Their experimental measurements of the photorefractive gain on CdTe: V show that the highest gains ($12cm^{-1}$ for a field amplitude of 10kV cm^{-1} at 1,32 µm) are obtained with a square-shaped periodic field at an optimum frequency (Fig. 5). Numerical calculations of the gain obtained by Ifegous et al [5] on CdTe: V permit reproduction of the experimental results (Fig. 5) especially the value of the optimal frequency and decrease of the photorefractive gain. This frequency behavior is explained by the charge model at two deep levels [5].

In this work, we present a charge model to $BaTiO_3$: Rh [6], we show that our numerical calculations based on this model allowed us to have the same frequency behavior with a very large photorefractive gain compared to the gain in the case of CdTe: V.

II. NUMERICAL SIMULATION OF THE EVOLUTION OF THE GAIN

2.1 Physical approach: Three state-of-charge model applied to BaTiO3: Rh at λ = 850nm

Chemical analysis of $BaTiO_3$: Rh crystals revealed that rhodium occurs in three charge states: Rh^{3+}, Rh^{4+}, Rh^{5+}. Two levels are involved :$Rh^{3+/4+}$ and $Rh^{4+/5+}$. In this material, conduction is due to the holes that exist in the valence band [6].

The process of charge transfer is therefore written in the form:

$$Rh^{5+} \Leftrightarrow Rh^{4+} + p$$
$$Rh^{4+} \Leftrightarrow Rh^{3+} + p$$

Where p denotes a free hole.

This model is said to be "three state of charge". As Rh^{4+} and Ti^{4+} have the same state of charge, we consider that Rh^{4+} has a state of charge "neutral " and its volume density will be denoted by N. As a result, Rh^{3+} appears as a hole acceptor and Rh^{5+}as a hole donor. Their respective volume densities will be denoted N^- and N^+. The electrical neutrality of the material is ensured by constant volume densities N_A (electron acceptors) and N_D (electron donors). The proposed diagram for this model is shown in figure 1.

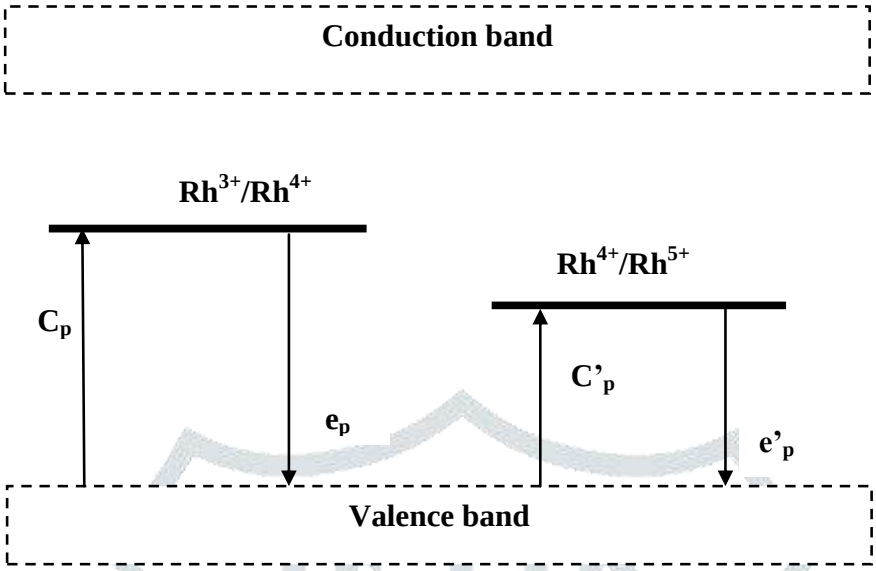

Figure 1: Three-band state-of-charge model applied to $BaTiO_3$: Rh [6].

Cp and C'_p are respectively the coefficients of recombination of the holes in the levels Rh^{4+} and Rh^{5+}, e_p and $e'_p$are the emission rates of the holes of these same levels.

The total volume density of rhodium in the material denoted N_T (density of traps):

$$N_T = N^- + N + N^+ \quad (1)$$

The equations governing the photorefractive effect are :

Continuity equations

$$\frac{\partial N^-}{\partial t} = e_p N - C_p p N^- \quad (2)$$

$$\frac{\partial N^+}{\partial t} = -e'_p N^+ + C'_p p N \quad (3)$$

With:

$$e_P = e_p^{th} + \sigma_p^0 I \quad (4)$$

$$e'_p = e_p^{th\prime} + \sigma_p^{0\prime} I \quad (5)$$

Here,

p : the density of holes.

e_p and e_p' : the hole emission rate from Rh^{4+} and Rh^{5+} levels to the valence band.

e_p^{th} and e_p^{th}' : the thermal emission rate of holes from Rh^{4+} and Rh^{5+}levels to the valence band.

C_p and C_p': the rates of recombination of holes in Rh^{4+} and Rh^{5+}.

$\sigma^0{}_p$and$\sigma_p{}^{0'}$: the photoionisation cross section from the Rh^{4+} and Rh^{5+}levels.

I : the illumination intensity.

Transport equations

$$J_P = p\, e\, \mu_p\, E - eD_P \frac{dp}{dx} \quad (6)$$

Such as :

$$D_P = \frac{K_B T}{e} \mu_p \quad (7)$$

e : (positive) charge of the hole.

p : mobility of the hole.

k_B: Boltzmann constant.

T : absolute temperature.

D_P : hole diffusion coefficient.

These equations are completed by the Poisson equation, which gives the spatial variation of the internal electric field:

$$\frac{dE}{dx} = \frac{e}{\varepsilon}(N_D - N_A + p + N^+ - N^-) \quad (8)$$

ε : Permittivity

In two beams coupling, two coherent waves interfere in a crystal under an angle 2θ and may exchange energy in the region where the beams overlap. When a weak signal beam gains intensity by depleting the pump beam, this creates an "optical amplification". The importance of the photorefractive effect can be estimated from the measurement of this amplification (photorefractive gain). According to the dynamic two-wave coupling theory, the gain coefficient Γ is expressed by:

$$\Gamma = \left[\frac{2\pi n_0^3 r_{eff}}{\lambda \cos\theta}\right]\left[\frac{\mathrm{Im}\{E_1\}}{m}\right] \quad (9)$$

n_0 : the refractive index.
r_{eff} : the effective electro-optic coefficient.
λ : the wavelength.
E_1: the complex amplitude of space-charge field.
m : the fringe modulation ratio.
Based on the fundamental equations (Poisson equation, transport equations, continuity equations, densities of traps ....) and approximations (adiabatic approximation, approximations on time constants ...) we have obtained the evolution equation of space charge field E_1 in the presence of an external square shaped field E_0 :

$$\tau'_{Ip}\tau_g\frac{d^2E_1}{dt^2} + \tau_g\frac{dE_1}{dt} + E_1 = mE_{SC} \quad (10)$$

With

$$E_{SC} = -i\frac{e}{K\varepsilon}I_0\frac{-\frac{\left[\frac{1}{\tau_{Dp}}+\frac{i}{\tau_{Ep}}\right]}{\left[\frac{1}{\tau_{Rp}}+\frac{1}{\tau_{Dp}}+\frac{i}{\tau_{Ep}}\right]}(\sigma_p^0 p_{T0} + \sigma_p^{0'} p'_{T0})}{\frac{1}{\tau_{di,p}} + \frac{\left[\frac{1}{\tau_{Ip}}-\frac{i}{\tau_{di,p}}\right]\left[\frac{1}{\tau_{Dp}}+\frac{i}{\tau_{Ep}}\right]}{\left[\frac{1}{\tau_{Rp}}+\frac{1}{\tau_{Dp}}+\frac{i}{\tau_{Ep}}\right]}} \quad (11)$$

Here, τ_{Ip}' is the time-constant of exchange between the Rh^{5+} level and the valence band, τg is the grating formation time constant, and Esc is the saturated space-charge field.
The symbols used in Eq. 11 are holes densities in the Rh^{4+} and Rh^{5+} levels p_{T0}, p'_{T0}; time-constant of relieving dielectric under illumination $\tau_{di;p}$; time-constant of exchange between the Rh^{5+} level and valence band τ_{Ip}; diffusion time-constant τ_{Dp}; drift time-constant τ_{Ep}; recombination time-constants in the Rh^{4+} level τ_{Rp}; photoionisation cross section from the Rh^{4+} and Rh^{5+} levels $\sigma^0_{p,}$ $\sigma_p^{0'}$; grating vector module K; electron charge e; and illumination I_0.
By following the same calculation steps in the case of CdTe: V for the deep two-level model we found the following equation [5]:

$$\left[\frac{\tau'_{In}\tau'_{Ip}}{\tau'_{In}+\tau'_{Ip}}\right]\tau_g\frac{d^2E_1}{dt^2} + \tau_g\frac{dE_1}{dt} + E_1 = mE_{SC} \quad (12)$$

τ_{In}' is the time-constant of exchange between the second level and the conduction band.
By comparing Eq. 10 with Eq. 12, we notice that the terms which take into account the interaction between the levels and the conduction band disappear in Eq. 10, because in our model, in the energy-level diagram (Fig.1), there is no interaction between the two levels and the conduction band.

2.2. Mathematical and numerical approach:

Eq. 10 looks like a second order differential equation. So, we can write it in the following form:

$$\frac{1}{\alpha+i\beta}\frac{d^2E_1}{dt^2} + \frac{1}{\gamma+i\delta}\frac{dE_1}{dt} + E_1 = mE_{SC} \quad (13)$$

Where α, β, γ and δ are evaluated from physical parameters.

It is a question of programming a second order differential equation. We replace in Eq. 13 the first and second derivatives using the Taylor development, we obtain the following equation:

$$K_1E_1(t+\Delta t) + K_2E_1(t) + K_3E_1(t-\Delta t) + K_4 = 0 \quad (14)$$

Where :

$$K_1 = \frac{[2\alpha(\gamma^2+\delta^2)+\gamma(\alpha^2+\beta^2)\Delta t] + i[-2\beta(\gamma^2+\delta^2)-\delta(\alpha^2+\beta^2)\Delta t]}{2(\alpha^2+\beta^2)(\gamma^2+\delta^2)\Delta t^2} \quad (15)$$

$$K_2 = \frac{[(\alpha^2+\beta^2)\Delta t^2 - 2\alpha] + i2\beta]}{(\alpha^2+\beta^2)\Delta t^2} \quad (16)$$

$$K_3 = \frac{[2\alpha(\gamma^2+\delta^2)-\gamma(\alpha^2+\beta^2)\Delta t] + i[-2\beta(\gamma^2+\delta^2)+\delta(\alpha^2+\beta^2)\Delta t]}{2(\alpha^2+\beta^2)(\gamma^2+\delta^2)\Delta t^2} \quad (17)$$

$$K_4 = -m(E_{scr} + iE_{sci}) \quad (18)$$

Recurrent Eq.14 expresses E_1 (t) as a function of E_1 (t + Δt) but also as a function of E_1 (t-Δt). To avoid this problem, we introduce a new equation:

$$E_1(t) = Y(t)\,E_1(t+\Delta t) + W(t) \quad (19)$$

Where :

$$Y(t) = \frac{-K_1}{K_2 + K_3\,Y(t-\Delta t)} \quad (20)$$

$$W(t) = \frac{-K_3\, W(t-\Delta t) - K_4}{K_2 + K_3\, Y(t-\Delta t)} \quad (21)$$

After a rearrangement, Eq.13 is reduced to a system of recurrent equations:

$$E_1(t+\Delta t) = \frac{E_1(t) - W(t)}{Y(t)} \quad (22)$$

$$Y(t+\Delta t) = \frac{-K_1}{K_2 + K_3\, Y(t)} \quad (23)$$

$$W(t+\Delta t) = \frac{-K_3\, W(t) - K_4}{K_2 + K_3\, Y(t)} \quad (24)$$

This system of equations makes it possible to calculate E_1 at time $(t + \Delta t)$ knowing E_1, Y and W at time t.
The calculation of E_1 is carried out by iteration according to the following diagram:

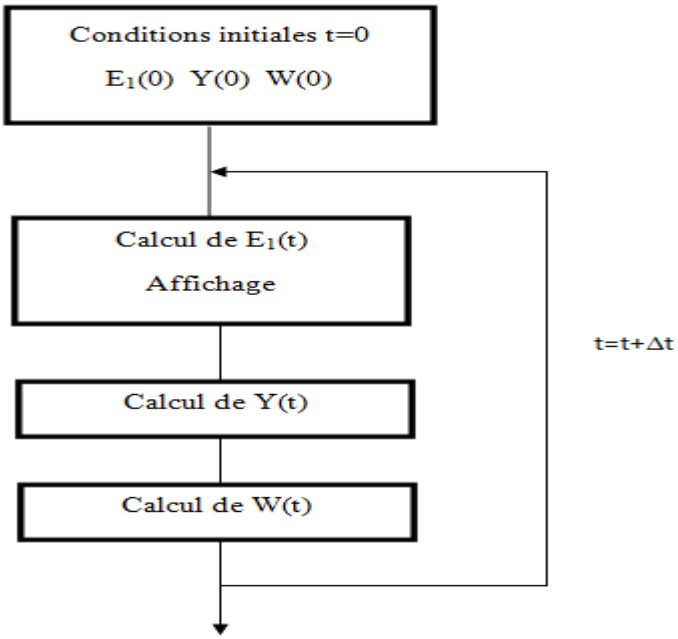

Figure 2 : Differential equation algorithm

III. RESULTS AND DISCUSSIONS

Our program allowed us to plot the gain in the complex plane and the gain versus time for different frequencies.
In the complex plane, one notices for the low frequencies (Fig.3: f = 10Hz), an important real part of the space charge field. By increasing the frequency (Fig.3: f = 30Hz), the gain increases and oscillates around the imaginary part of the space charge field. For frequencies above 30Hz, the oscillation disappears and the gain decreases (Fig.3: f = 400Hz and f = 1000Hz).
For the obtained results of the gain versus time (Fig. 4), we are notice that for low frequencies, a strong transient is obtained with a low amplitude of the gain (negative gain due to a loss of the photorefractive effect). As the frequency is increased, the gain increases to its maximum (Fig.4: f = 30Hz). Beyond this frequency (optimum frequency) the gain drops. These results are grouped together in the figure 5.

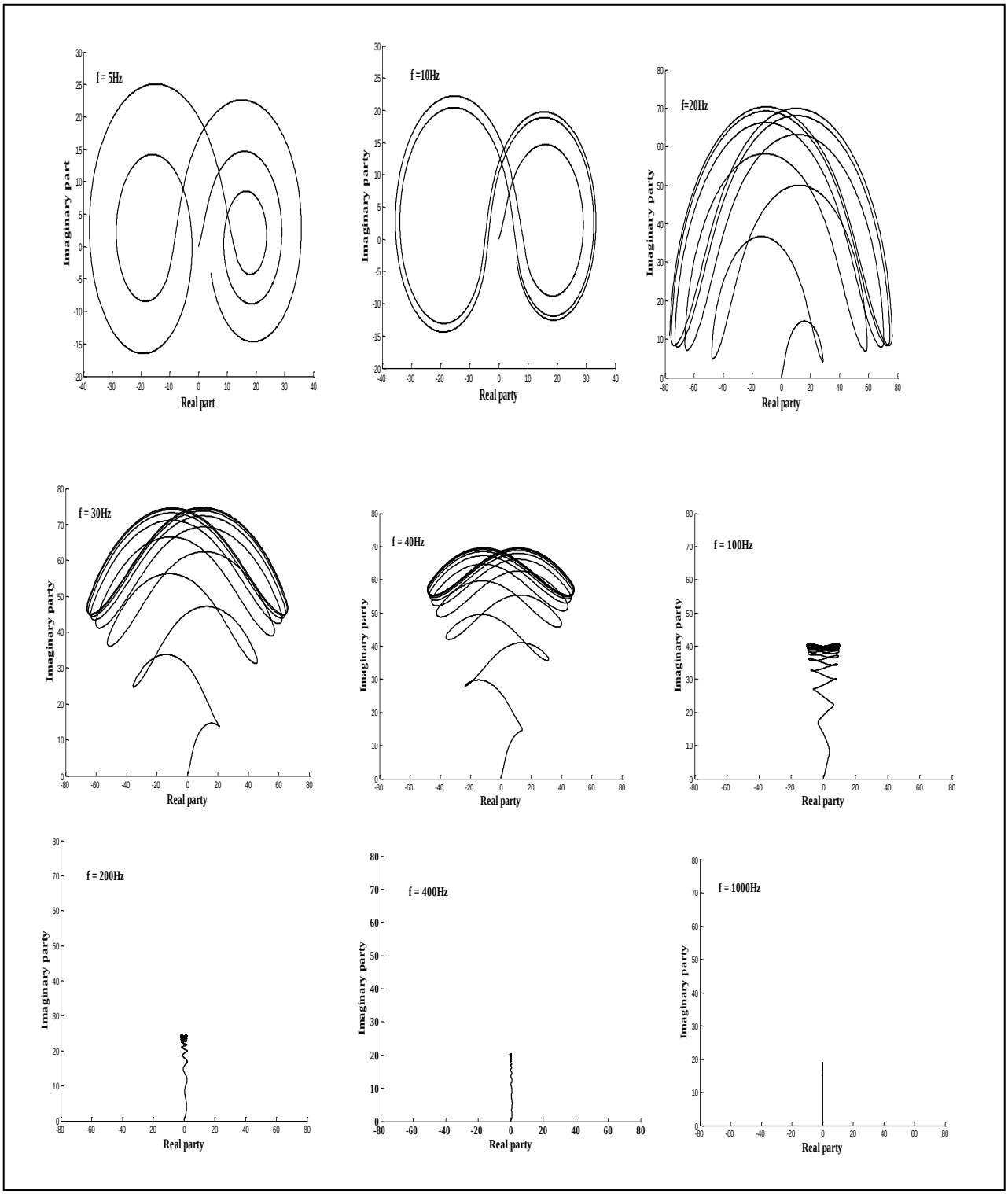

Figure 3: The evolution gain in the complex plane for different frequencies in $BaTiO_3$: Rh

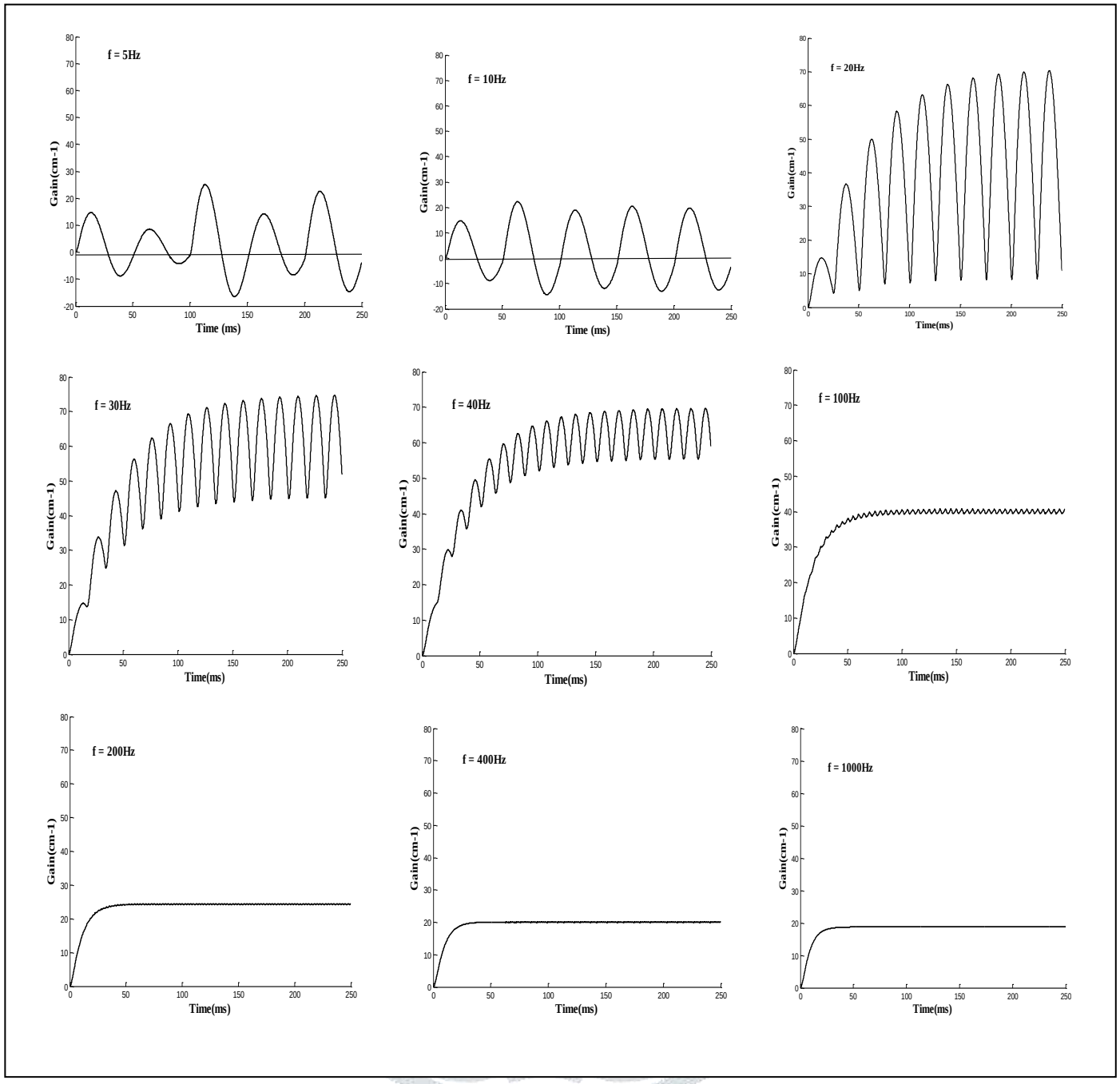

Figure 4 : The evolution gain versus time for different frequencies in $BaTiO_3$: Rh

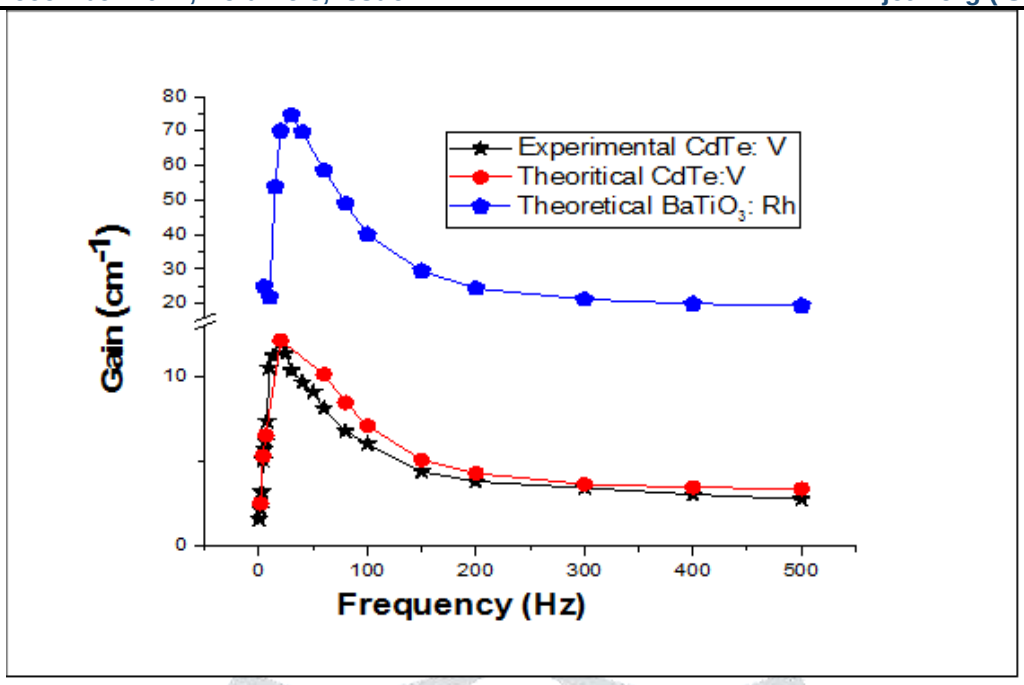

Figure 5: Gain versus frequency of the square shaped alternative electric field in CdTe: V (Experimental curve, Theoretical curve) and BaTiO3: Rh Theoretical curve.

We observe of an excellent gain and the existence of an optimum low frequency region in which the photorefractive gain is maximum. By comparing these results with those obtained for CdTe: V [5].We notice, that CdTe: V and $BaTiO_3$: Rh have the same frequency behavior, i.e. the existence of an optimal frequency for which the gain is maximum and beyond this frequency the gain is reduced (CdTe: V; f = 20Hz and $BaTiO_3$: Rh; f = 30Hz) and $BaTiO_3$: Rh has an excellent gain (Γ= 74,67 cm^{-1}) while CdTe: V (Γ= 12cm^{1}). Which shows that $BaTiO_3$: Rh is a good candidate for the photorefractive effect.

IV. Conclusion

Transport model with three states of charge applied to $BaTiO_3$: Rh at λ= 850 nm (near infrared) allowed us to have a evolution equation of space charge field in the presence of an external square shaped field (Eq. 10). Its numerical resolution resulted in a very high photorefractive gain (six times greater than that of CdTe: V**)**. Also an optimal frequency for which the gain is maximum. This frequency behavior has been found for other material such as CdTe: V, which makes $BaTiO_3$: Rh a good candidate for the photorefractive effect in telecommunications. A good mastery of the behavior of the $BaTiO_3$: Rh will then make it possible to optimize its performance.

References

[1] Andreea, C. Cernea, M. Corina, E. Aldica, G. Ganea, P. and Trusca, R. 2017. Lanthanum influence on the structure, dielectric properties and luminescence of $BaTiO_3$ ceramics processed by spark plasma sintering technique. Journal of Alloys and Compounds, vol. 706, pp. 538–545.

[2] Cao, J. Ji, Y. Tian, C. and Yi, Z. 2014. Synthesis and enhancement of visible light activities of nitrogen-doped BaTiO 3. Journal of Alloys and Compounds, vol. 615, pp. 243–248,

[3]Olatunji, Sunday O. andOwolabi, Taoreed O. 2021. Barium Titanate Semiconductor Band Gap Characterization through Gravitationally Optimized Support Vector Regression and Extreme Learning Machine Computational Methods. Mathematical Problems in Engineering Volume 2021, Article ID 9978384.

[4] Tian, M. Han, A. Ma, S. Zhu, X. Ye, M. and Chen, X. 2021. Preparation of Cr-doped BaTiO3 near infrared reflection pigment powder and its anti-aging performance for acrylonitrile-styrene-acrylate. Powder Technology, vol. 378, pp. 182–190.

[5] Ifegous, B. Fliyou, M. Adhiri, R. Sribi, C. Fahli, A. Souifi, A. and Bremond, G. 2002. Numerical simulation of photorefractive gain in CdTe:V with optimum frequency of the electric field. J.CrystalGrowth 240, 190-195.

[6] Bahssine, S. 2002. Caractérisation optique et électro-optique des cristaux photoréfractifs $BaTiO_3$ dopés Rh ($BaTiO_3$:Rh) et $Ba_xCa_{1-x}TiO_3$ dopés rhodium. Université de Metz.

[7] Moisan, J.Y. Wolfeer, N. Moine, O. Gravey, P. Martel, G. Aoudia, A. Rzepka, E. Marfaing, Y. Triboulet, R. 1994. J. Opt. Soc. Am. B 11. 1655.

[8] Zerrai, A. Marrakchi, G. Bremond, G. Moisan, J.Y. Martel, G. Gauneau, M. Lambert, B. Gravey, P. Wolffer, N. Aoudia, A. Marfaing, M. Triboulet, R. Koebel, J.M. Hage-Ali, M. Siffert, P. 1996. J. Crystal Growth 161, 264.